Surface & Coatings Technology 284 (2015) 75–79

Contents lists available at ScienceDirect

Surface & Coatings Technology

journal homepage: www.elsevier.com/locate/surfcoat

Effects of annealing on near-infrared shielding properties of Cs-doped tungsten oxide thin films deposited by electron beam evaporation

Chak Seng Long [a], Horng-Hwa Lu [b,*], Ding-Fwu Lii [c], Jow-Lay Huang [a,d]

[a] Department of Materials Science and Engineering, National Cheng Kung University, Tainan 701, Taiwan
[b] Department of Mechanical Engineering, National Chin-Yi University of Technology, Taichung 41170, Taiwan
[c] Department of Electrical Engineering, Cheng Shiu University, Kaohsiung 833, Taiwan
[d] Department of Chemical and Materials Engineering, National University of Kaohsiung, Kaohsiung 81148, Taiwan

ARTICLE INFO

Article history:
Received 1 April 2015
Revised 6 June 2015
Accepted in revised form 9 June 2015
Available online 26 July 2015

Keywords:
Tungsten bronze
Cs_xWO_3
Near-infrared shielding
Optical properties

ABSTRACT

Near-infrared (NIR) shielding properties are important for solar films. In this study, Cs_xWO_3 films prepared using electron beam evaporation were characterized using X-ray diffraction, X-ray photoelectron spectroscopy, and spectrophotometry. The effects of annealing on NIR shielding properties and film microstructure were investigated. The results show that the NIR shielding properties of Cs_xWO_3 films can be improved by annealing at 300–450 °C under pure H_2 atmosphere, the amorphous thin films being transformed to crystalline films. The Cs_xWO_3 films annealed at 450 °C in pure H_2 atmosphere showed high transmittance of visible light (70%) and high NIR shielding ratio (99%).

1. Introduction

Near-infrared (NIR) light shielding materials have been applied in solar collectors, smart windows, and optical filters [1–3]. NIR shielding has been achieved by utilizing transparent thermal coatings on windows. In summer, transparent thermal insulation coatings, which have excellent visible light transmittance, prevent heat transmission from the outside to the inside reducing air conditioning usage and, thus, energy consumption [4,5]. Transparent thermal insulation coatings can also be used as a solar filter. Transparent conductive oxides (TCOs) include indium tin oxide (ITO) and antimony tin oxide (ATO) [6]. Tungsten bronzes have received a lot of attention due to their electrochromic, photochromic, gasochromic, and superconducting properties [7–11]. Tungsten bronzes M_xWO_3 with dopant ions such as Na, K, Rb, Cs, and other alkali metals [12,13] have been found to have the best optical and electrical properties. Takeda et al. [14] found that cesium tungsten bronze (Cs_xWO_3) film has excellent NIR absorption and shielding properties. One study [15] found that Cs_xWO_3 has a strong NIR shielding ability as well as high transparency in the visible light region. Cs_xWO_3 with a hexagonal structure exhibited higher NIR shielding than that of ITO, and is thus a possible replacement for ITO and ATO in windows. Cs_xWO_3 powders have mainly been synthesized via the solvothermal reaction method [16–18] or hydrothermal reaction method [19–21] before being coated onto substrates. The present study is aimed at the investigation of the H_2 annealing effects on the microstructure, morphology and NIR shielding properties of the Cs_xWO_3 films prepared by electron beam evaporation.

2. Experimental Procedure

Thin films of Cs_xWO_3 were deposited on quartz glass via electron beam evaporation. The source material was Cs_xWO_3 ($0 < x < 1$) powders. (NanoStar Technology Co). The substrates were cleaned with acetone and methanol by treatment for 10 min in each solvent. Then, the substrates were washed with isopropyl alcohol and deionized water for 10 min. The electron gun was operated at 8 kV and 10 mA. The evaporation was carried out for 40 min at a base pressure of 7.5×10^{-6} Torr. The films were grown at a constant temperature (273 K). The thickness of the Cs_xWO_3 films was controlled to be 280 nm with deposition at a constant rate of 3 Å · s^{-1} using an in situ quartz crystal thickness monitor. The phase composition and crystallinity of the Cs_xWO_3 film were determined using X-ray diffraction (XRD) analysis (Rigaku DMAX 2500) with Cu Kα radiation ($\lambda = 1.54$ Å) at a scan speed of 1°/min. Ultrahigh-resolution field-emission scanning electron microscopy (UHRFE -SEM; ZEISS SUPRA series) and energy-dispersive X-ray spectroscopy (EDX) analysis were performed. The binding energies of tungsten core levels in the Cs_xWO_3 film were determined using X-ray photoelectron spectroscopy (XPS; VersaProbe PHI 5000). The morphology of the film was determined using field-emission SEM (Hitachi-4800). The optical transmittance spectra were measured at room temperature (RT) using ultraviolet/visible/NIR spectrophotometry

* Corresponding author.
E-mail address: hhlu@ncut.edu.tw (H.-H. Lu).

http://dx.doi.org/10.1016/j.surfcoat.2015.06.078
0257-8972/

(Hitachi U-4100) in the wavelength range of 260-2600 nm. The surface morphology of the deposited film was observed using atomic force microscopy (AFM; Veeco CP-II) in semi-contact mode with Si tips at a scan rate of 1 Hz.

3. Results and Discussion

3.1. Microstructure of films

Fig. 1 shows SEM images of Cs_xWO_3 thin films before and after H_2 annealing at 300-500 °C. No obvious precipitates or impurities appear on the surface of the $Cs_{0.32}WO_3$ thin films (Fig. 1(a)). Fig. 1(b) and (c) show no distinct variation in the surface morphology of the thin films after annealing. However, when the annealing temperature was 400 °C, the grain size increased (Figs. 1(d) and (e)).

Fig. 2 shows three-dimensional (3D) AFM images (scanning area: 3 μm × 3 μm) of Cs_xWO_3 thin films deposited at various annealing temperatures. The films deposited at RT had a relatively smooth surface with vague grain boundaries, as shown in Fig. 2(a). The roughness was found to be 0.95 nm and the surface was continuous. The surface roughness and grain size increased with increasing annealing temperature. As shown in Figs. 2(b) and (c), when the annealing temperature was increased from 300 to 350 °C, the surface roughness increased from 1.55 to 1.73 nm. The surface roughness increased from 2.15 nm (400 °C) to 4.77 nm (450 °C). The grain size increase with annealing temperature is attributed to atomic rearrangement (atoms move faster on the surface of the films at higher temperature).

3.2. Phase composition of films

Fig. 3 shows XRD patterns of Cs_xWO_3 thin films before and after H_2 annealing at 300-450 °C for 2 h. Fig. 3(a) shows XRD patterns of as-deposited $Cs_{0.32}WO_3$ thin films. The diffraction peak absence indicates the amorphous film state. Figs. 3 (b-e) show XRD patterns of films annealed at 300, 350, 400, and 450 °C for 2 h, respectively. The Cs_xWO_3 thin film crystallization is found after treatment at 300 °C. The characteristic peaks of the Cs_xWO_3 thin films corresponded to the (002), (200), (112), (202), (212), (220), (204), (312), (400), and (224) planes. This agrees well with hexagonal $Cs_{0.32}WO_3$ (JCPDS card no. 831334). No impurity peaks appeared. With increasing annealing temperature, the diffraction peaks became more apparent and sharper. It was reported that Cs ions (0.170 nm) can occupy hexagonal vacant tunnels (0.163 nm) in the hexagonal tungsten bronze structure [1]. The grain size, D, of the crystallites was calculated using Scherrer's formula:

$$D = \frac{K\lambda}{\beta \cos\theta}$$

where K is the Scherrer constant (= 0.9), λ is the wavelength of the X-ray (= 1.54 Å for Cu Kα radiation), θ is the Bragg angle, and β is the line broadening at half the maximum intensity (full width at half maximum). The grain size, D, increased from 15 to 30 nm when the annealing temperature was increased from 0 to 400 °C. The initially amorphous $Cs_{0.32}WO_3$ thin films gradually crystallized with increasing H_2 annealing temperature. This result is consistent with the SEM and AFM images in Figs. 1 and 2.

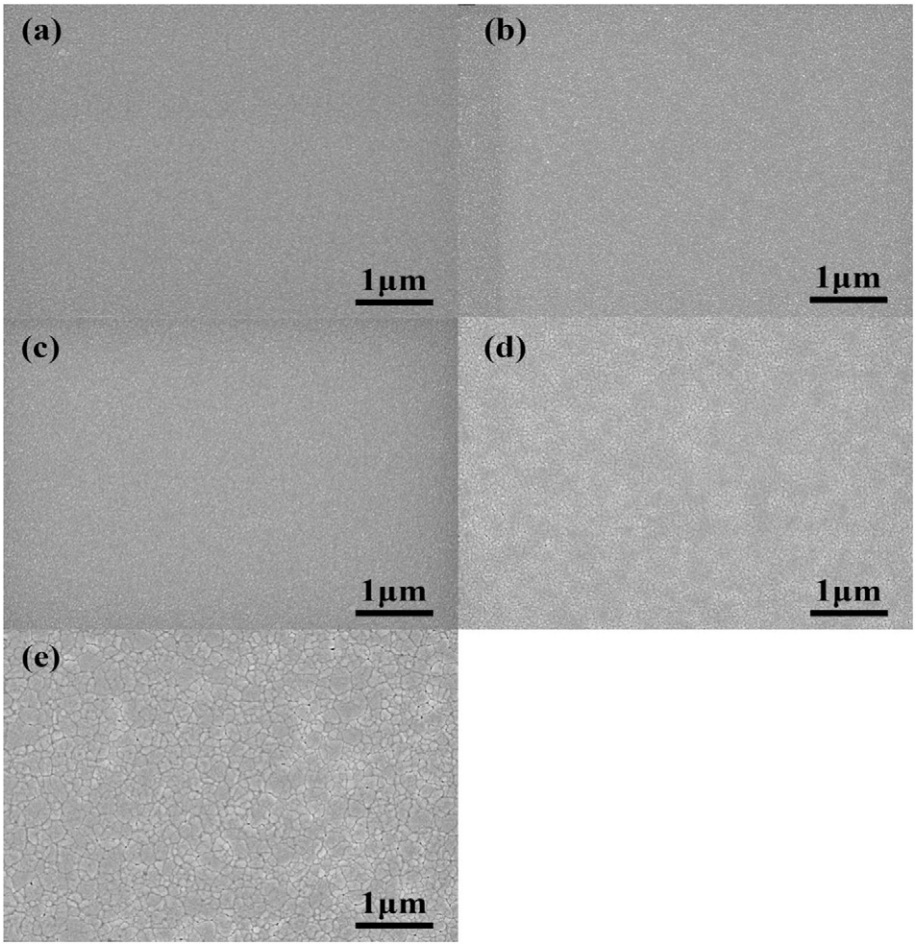

Fig. 1. SEM images of (a) as-sputtered $Cs_{0.32}WO_3$ films and those annealed at (b) 300 °C, (c) 350 °C, (d) 400 °C, and (e) 450 °C.